

# Polyaniline Nanoparticles Prepared by Micro-Emulsion Polymerization for Corrosion Inhibition of Carbon Steel in 1M HCl

Rania E. Morsi<sup>1</sup>, E.A. Khamis<sup>2</sup>

<sup>1,2</sup>Egyptian Petroleum Research Institute, Nasr City, P.B. 11727, Cairo, Egypt

**Abstract:** Polyaniline nanoparticles were prepared using oxidation polymerization in micro-emulsion system. Sodium dodecyl sulphate was used as a surfactant which dissolved in hydrochloric acid giving the micellar solution. Potassium persulphate was used as an oxidant. The produced particles were spherical in shape with an average diameter of 15 nm as detected from the transmittance electron microscope images. Polyaniline nanoparticles were investigated as corrosion inhibitors using electrochemical measurements. It has been found that nanopolyaniline is an efficient inhibitor, since the maximum efficiency of 94% has been observed at a concentration of 500 ppm.

**Keywords:** Polyaniline, nanoparticles, electrochemical measurements, corrosion

## 1. Introduction

Corrosion of the metals is one of the most serious problems that mankind has to face [1]. Conducting polymers as either film forming corrosion inhibitors or in protective coating have attracted more and more attention due to the excellent anticorrosion ability and environmental friendship [2]. Among conducting polymers, polyaniline (PANI) is generally recognized to be one of the best candidate for an anti-corrosion coating, because of its ease of preparation, excellent environment stability, and interesting redox properties associated with the chain of nitrogens [3–6].

Polyaniline is one of the important conducting polymers which has been studied extensively for various applications such as sensors, transparent conductor, ESD and EMI protection, electrochromic displays etc. [7]. This polymer has been found to be an important constituent in coatings and recently that it has drawn attention as an effective material for corrosion protection [8–13]. Corrosion is a natural process that has troubled human beings ever since the use of metals. It occurs because metals tend to return to their more stable oxidized states; that is, the corrosion of a metal occurs when its potential has a value more noble than the reversible potential. Due to the strict regulations on the usage of heavy metals as the additive, the search of an effective organic corrosion inhibitor in replacement of those metal ones has become essential. For more than a decade, polyaniline (PANi) has been used in protecting metals because of its unique properties. PANi is unique in that it has a nitrogen heteroatom incorporated between phenyl rings along polymer chain. This structure provides flexibility and allows the existence of three distinguished oxidation states that are leucoemeraldine, emeraldine, and pernigraniline. Leucoemeraldine and pernigraniline forms of PANi are not stable, and they will return to the state of emeraldine under the atmospheric environment.

## 2. Experimental

### 2.1 Materials

Aniline (Merck) was purified by vacuum distillation before polymerization. All other reagent are of analytical grade and used without further purification.

### 2.2. Polyaniline micro-emulsion polymerization

The material was prepared by microemulsion polymerization in acidic sodium dodecylsulfate (SDS) as micellar solution. Sodium dodecyl sulphate (4.32 grams) was dissolved in 0.1 M HCl (100 ml) solution. The monomer; aniline (0.28 grams), was added drop-wise to the micellar surfactant solution under continues stirring until a transparent microemulsion is formed. Then, potassium persulphate as an oxidant (in molar ratio of 0.5 with respect to aniline) was added drop-wise to the previously prepared emulsion and kept at 200C under stirring for a period of 60 minutes while which the homogeneous transparent reaction mixtures turned into blue and its coloration was pronounced as polymerization proceeded.

### 2.3 Characterization

The samples were characterized by powder X-ray diffraction (XRD) using a Philips X'Pertpro Pan-analytical instrument. Data was taken for the  $2\theta$  range of 10 to 100 degrees with a step of 0.02 degree. High Resolution Transmission Electron Microscopy (HR-TEM) imaging was performed using a Jeol-JEM Japan 2100 operating at 200 kV, the samples for TEM were prepared by making sonication for samples in ethyl alcohol and depositing onto a copper coated carbon grid and then let the solvent to evaporate.

### 2.4 Solutions

The aggressive solution, 1M HCl, was prepared by dilution of analytical grade, 37% HCl with distilled water. The concentration range of polyaniline nanoparticles was from

100 to 500 ppm used for corrosion measurements. All solutions were prepared using distilled water.

### 2.5 Electrochemical measurements

Carbon steel working electrode of the following chemical composition (wt. %) was used in the experiments: 0.07% C, 0.24% Si, 1.35% Mn, 0.017% P, 0.005% S, 1006% Cr, 1008% Ni, 1002% Mo, 0.01% Cu and the remainder Fe. A pre-treatment was carried out prior to each experiment, in which specimen surface was mechanically ground with 400, 600, 800 and 1000 emery paper, washed with acetone and bidistilled water then dried and put into the cell [14]. The electrochemical measurements were carried out using Volta lab 40 (Tacussel-Radiometer PGZ301) potentiostat and controlled by Tacussel corrosion analysis software model (Voltmaster 4) at under static condition. The corrosion cell used had three electrodes. The reference electrode was a saturated calomel electrode (SCE). A platinum electrode was used as auxiliary electrode. All potentials given in this study were referred to this reference electrode. The working electrode was immersed in test solutions for 30 minutes to an establish steady state open circuit potential ( $E_{ocp}$ ). After measuring the  $E_{ocp}$ , the electrochemical measurements were performed. The polarization curves were obtained in the potential range from -850 to -350m V(SCE) with a 2 mVs-1 scan rate. Electrochemical impedance spectroscopy (EIS) measurements

were carried out as described elsewhere [15]. A small alternating voltage perturbation (5 mV) was imposed on the cell over the frequency range of 100 kHz to 30 mHz at open circuit potential. Each experiment was repeated for at least three times to check the reproducibility.

## 3. Results and discussion

Polyaniline (PANI) is one of the promising polymers due to its low cost, ease of preparation, good thermal and electrical properties, its environmental stabilities, and versatile applications [16]. It possesses exceptional structural properties due to the inception of nitrogen heteroatom between the phenyl rings along the polymer backbone. polyaniline (PANI) possesses a large amount of amine and imine functional groups which allow its use in specific applications. Moreover, nano-scale polyaniline with large specific surface areas have higher applicability than the regular scale ones.[17]

Among different methods of Polyaniline synthesise, the chemical oxidation is the widely used most prominent one. The chemical oxidation polymerization is practically viable due to feasibility of synthesis mechanism and low cost of production. Powder nanotubes can be prepared directly by oxidation polymerization method without using any templates or acids.[18] Another facile method of synthesizing PAN is microemulsion polymerization containing a large amount of nanoscopic micelles which can align and absorb the monomer and adjusting polymerization reaction, to yield polymer microspheres with improved properties.[19] Polyaniline/ water based dispersion is attractive alternatives which could utilize the use of the produced stable dispersed nanoparticles. Furthermore, it

possesses some special properties of the nanoparticles. For applications, this kind of materials is suitable to be used as corrosion protective ones, which is much better than the coatings based on organic solvent or strong acid due to the environment perspectives.

### 3.1 Preparation of polyaniline nanoparticles

The main typical bands of polyaniline nanoparticles, represented in Figure 1, are assigned as follow; the bands at 829 and 1145 cm-1 are due to the aromatic C-H in-plane bending and the out-of-plane deformation of C-H in the 1, 4-disubstituted benzene ring. The C-H out-of-plane bending vibrations band from a para-substitution pattern at 829 cm-1 and the N Q N absorption peak at 1145 cm-1 (with Q representing the quinoid ring) indicate the head-to-tail coupling of aniline monomers[20]. The main chain characteristic bands at 1507 and 1588 cm-1 was attributed to the C=N and C=C stretching modes for the quinoid and benzenoid rings, respectively. Bands at 1300 and 690 cm-1 can be assigned to C-N stretching of the secondary aromatic amine and aromatic C-H out-of plane bending vibrations, respectively. The broad bands in the range of 3000–3500 cm-1 correspond to secondary amine stretching (N-H) vibrations [21]

Figure 2 shows the X-ray diffraction of PANI nanoparticles. The diffraction patterns consisted of broad crystalline peaks and the prominent peak about  $2\theta = 18.55^\circ$  can be attributed to the periodicity parallel to the polymer chain, whereas the peak around  $2\theta = 25.8^\circ$  is attributed to the periodicity perpendicular to the direction of polymer chain indicating the predominant amorphous structure of the polymer chain.[20] In particular, the unusual peak around  $2\theta = 10.83^\circ$  may be assigned to the scattering along the orientation parallel to the polymer chain.[22]

Polyaniline nanoparticles were investigated by high-resolution transmission electron microscope (HR-TEM), as shown in Figure 3. The morphology of PANI was spherical nanoparticles with average diameter of 15 nm.

### 3.2 Potentiodynamic polarization measurements

Potentiodynamic polarization curves for carbon steel in 1M HCl without and with various concentrations of the nPAN from 100 to 500 ppm at 30°C are shown in **Figs. (1)**. The presence of corrosion inhibitor causes a prominent decrease in the corrosion rate i.e. shifts both anodic and cathodic curves to lower values of current densities. Namely, both cathodic and anodic reactions are drastically retarded by corrosion inhibitor in 1M HCl. Values of corrosion current densities ( $i_{corr}$ ), corrosion potential ( $E_{corr}$ ), cathodic Tafel slope ( $b_c$ ), anodic Tafel slope ( $b_a$ ), and inhibition efficiency ( $\eta_p$ ) were calculated and given in **Table 1**. The  $\eta_p$  was calculated from polarization measurements according to the relation given below;

$$\eta_p = \frac{i_{corr}(\text{unin h}) - i_{corr}(\text{in h})}{i_{corr}(\text{unin h})} \times 100 \quad (1)$$

where;  $i_{corr}(\text{uninh})$  and  $i_{corr}(\text{inh})$  are uninhibited and inhibited corrosion current densities, respectively.  $b_a$  and  $b_c$  values did not show significant changes, this result indicated that the

anodic and cathodic corrosion reaction mechanism did not change. Clearly,  $i_{\text{corr}}$  decreased remarkably while  $\eta_p$  increased with the increasing of the inhibitor concentration, and the maximum ( $\eta_p$ ) is 94.59% at 500 ppm. There is no definite trend in the shift of  $E_{\text{corr}}$  in the presence of corrosion inhibitor, therefore, the prepared inhibitors can be arranged as a mixed-type inhibitor, Amines in aqueous acidic solutions may exist as either neutral molecules or in the form of cations depending upon the concentration of  $H^+$  ions in the solutions. In acidic solutions, they predominantly exist as cations and adsorb through electrostatic interaction between the positively charged aniline cation and negatively charged metal surface [23]. Moreover, in aromatic amines, the interaction between  $\pi$  electrons of benzene ring and the positively charged metal surface also plays a role. The stronger adsorption of organic molecules is not always a direct combination of organic molecules with the metal surface, but in some cases, it occurs through already adsorbed sulfate ions, which will interfere with the adsorption of organic molecules [24].

### 3.3 Electrochemical impedance spectroscopy (EIS)

Corrosion behavior of carbon steel in 1M HCl in the presence and absence of the prepared inhibitors was investigated using EIS at 30 °C. Nyquist plots of carbon steel in 1M HCl solutions with and without different concentrations of inhibitors are given in **Figs. 2**. Plots revealed that the impedance response of carbon steel in 1M HCl was not significantly changed after adding the inhibitor compounds. The EIS spectrum of the nPAN was analyzed using the equivalent circuit as shown in **Fig. 3**. It represented a single charge transfer reaction and it fitted well with the obtained experimental results. The intersection of the capacitive loop with the real axis represented the ohmic resistance of the corrosion product films and the solution enclosed between the working and the reference electrode,  $R_s$  [25].  $R_{ct}$  represents the charge transfer resistance. It measures the electron transfer across the surface, which is inversely proportional to the corrosion rate [26]. Inhibition efficiency ( $\eta_i$ ) was calculated from the values of  $R_{ct}$  using the following equation [27, 28]:

$$\eta\% = (1 - R_{ct}^*/R_{ct}^*) \times 100 \quad (2)$$

where,  $R_{ct}^*$  and  $R_{ct}$  are the charge transfer resistance in the presence and absence of the nPAN, respectively. The double layer capacitance ( $C_{dl}$ ) was calculated using the following equation [29-31]:

$$C_{dl} = \frac{1}{2\pi f_{\text{max}} R_{ct}} \quad (3)$$

Where,  $f_{\text{max}}$  is the frequency of maximum imaginary components of the impedance. Various parameters such as charge transfer resistance ( $R_{ct}$ ), double layer capacitance ( $C_{dl}$ ), and inhibition efficiency ( $\eta_i$ ), were calculated and listed in **Table 2**. It is obvious that the charge transfer resistance ( $R_{ct}$ ) was increased, whereas the capacitance ( $C_{dl}$ ) was decreased with increasing the inhibitor concentration. The decrease in the capacitance, which can result from a decrease in local dielectric constant and/or an increase in the thickness of the electrical double layer, suggested that the inhibitor molecules had an adsorption act at the metal/solution interface. The addition of the prepared inhibitors resulted in lower  $C_{dl}$  values, which could be a

consequence of the replacement of water molecules by inhibitor molecules at the electrode surface. The inhibitor molecules may also reduce the capacitance by increasing the thickness of the double layer according to the Helmholtz model [32]:

$$\delta_{org} = \frac{\epsilon \epsilon_0 A}{C_{dl}} \quad (4)$$

where,  $\epsilon$  is the dielectric constant of the medium,  $\epsilon_0$  is the vacuum permittivity,  $A$  is the electrode surface area, and  $\delta_{org}$  is the thickness of the protective layer. The values of  $C_{dl}$  were smaller in the presence of the inhibitor than in its absence. This may be resulted from the effective adsorption of the nPAN.

## 4. Conclusion

- 1) Polyaniline nanoparticles were prepared using oxidation polymerization in micro-emulsion system. Sodium dodecyl sulphate was used as a surfactant which dissolved in hydrochloric acid giving the micellar solution.
- 2) The corrosion inhibition for carbon steel was studied in 1 M HCl using electrochemical techniques. It was obtained that the inhibitive efficiency of PANI increased with increasing concentration. PANI showed 94.59% inhibitive efficiency at 500ppm. The result revealed that nPAN was an efficient mix-type polymeric inhibitor which acted through adsorption mechanism.

## References

- [1] N. Ahmad, A.G. MacDiarmid, Synth. Met. 78 (1996) 103–110.
- [2] P. Chandrasekhar, Conducting Polymers, Fundamentals and Applications: a Practical Approach, Kluwer Academic Publishers, London, 1999.
- [3] A.G. MacDiarmid, Angew Chem. Int. Ed. 40 (2001) 2581–2590.
- [4] N. Gospodinova, L. Terlemezyan, Prog. Polym. Sci. 23 (1998) 1443–1484.
- [5] A. Ray, A.F. Richter, A.G. MacDiarmid, A.J. Epstein, Synth. Met. 29 (1989) 151–156.
- [6] A.H.L. Geoff, M.C. Bernar, Synth. Met. 60 (1993) 115–131.
- [7] L. Alcacer, Conducting Polymers, Riedel, Dordrecht, Holland, 1987.
- [8] A.J. Dominis, G.M. Spinks, G.G. Wallace, Prog. Org. Coat. 48 (2003) 43.
- [9] P.J. Kinlen, J. Ding, D.C. Silverman, Corrosion 58 (2002) 490.
- [10] N. Ahmad, A.G. MacDiarmid, Synth. Met. 78 (1996) 103.
- [11] P.J. Kinlen, D.C. Silverman, C.R. Jeffreys, Synth. Met. 85 (1997) 1327.
- [12] T. Schauer, A. Joos, L. Dulog, C.D. Eisenbach, Prog. Org. Coat. 33 (1998) 20.
- [13] C.K. Tan, D.J. Blackwood, Corros. Sci. 45 (2003) 545.
- [14] M. Palomar-Pardavé, M. Romero-Romo, H. Herrera-Hernández, M.A. Abreu-Quijano, Natalya V. Likhonova, J. Uruchurtu, J.M. Juárez-García, Corros. Sci. 54 (2012) 231–243.
- [15] M.A. Hegazy, A.S. El-Tabei, A.H. Bedair, M.A. Sadeq, Corros. Sci. 54 (2012) 219–230.

- [16] Ivana Šteđnková, Miroslava Trchova, Jaroslav Stejskal, Polymer Degradation and Stability 93 (2008) 2147–2157
- [17] Nina Jiang, Yiting Xu, Yuqiong Dai, Weiang Luo, Lizong Dai, Journal of Hazardous Materials 215–216 (2012) 17–24
- [18] Y.F. Huang, C.W. Lin, Synthetic Metals 159 (2009) 1824–1830.
- [19] Xin-Gui Li, Mei-Rong Huang, Jian-Feng Zeng, Mei-Fang Zhu Colloids and Surfaces A: Physicochem. Eng. Aspects 248 (2004) 111–120.
- [20] Y.F. Huang, C.W. Lin, Exploration of the formation mechanisms of polyaniline nanotubes and nanofibers through a template-free method, Synthetic Metals 159 (2009) 1824–1830.
- [21] Mohamad Ayad, Gad El-Hefnawy, Sawsan Zaghlool, Facile synthesis of polyaniline nanoparticles; its adsorption behavior, Chemical Engineering Journal 217 (2013) 460–465
- [22] Chien-Hsin Yang, Yi-Kai Chih, Hsyi-En Cheng, Cheng-Ho Chen, Nanofibers of self-doped polyaniline, Polymer 46 (2005) 10688–10698.
- [23] Gerovich, M. A.; Rybalchenko, G. F. ZhFizKhim 1958, 32, 109.
- [24] Antropov, L. I. 1st International Cong Metal Corrosion; Butterworths: London, 1963; p 147.
- [25] H.H. Hassan, E. Abdelghani, M.A. Amin, Electrochim. Acta 52 (2007) 6359–6366.
- [26] A.M. Abdel-Gabar, B.A. Abd-El-Nabey, I.M. Sidahmed, A.M. El-Zayady, M. Saadawy, Corros. Sci. 48 (2006) 2765–2779.
- [27] J.R. Macdonald, W.B. Johanson, in: J.R. Macdonald (Ed.), John Wiley & Sons, New York, 1987.
- [28] D.K. Yadav, M.A. Quraishi, B. Maiti, Corros. Sci. 55 (2012) 254–266.
- [29] M.A. Migahed, A.M. Abdul-Raheim, A.M. Atta, W. Brostow, Mater. Chem. Phys. 121 (2010) 208–214.
- [30] Khalid I. Kabel, Khaled Zakaria, Mohammed A. Abbas, E.A. Khamis, Journal of Industrial and Engineering Chemistry, (2014) In press.
- [31] R.F.V. Villamill, P. Corio, J.C. Rubim, S.M.L. Agostinho, J. Electroanal. Chem. 535 (2002) 75
- [32] M.A. Migahed, A.M. Abdul-Raheim, A.M. Atta, W. Brostow, Mater. Chem. Phys. 121 (2010) 208–214.

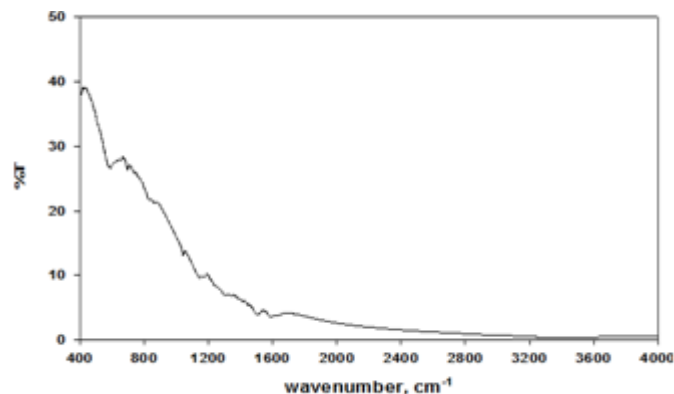


Figure 1. FT-IR spectra of the prepared polymers

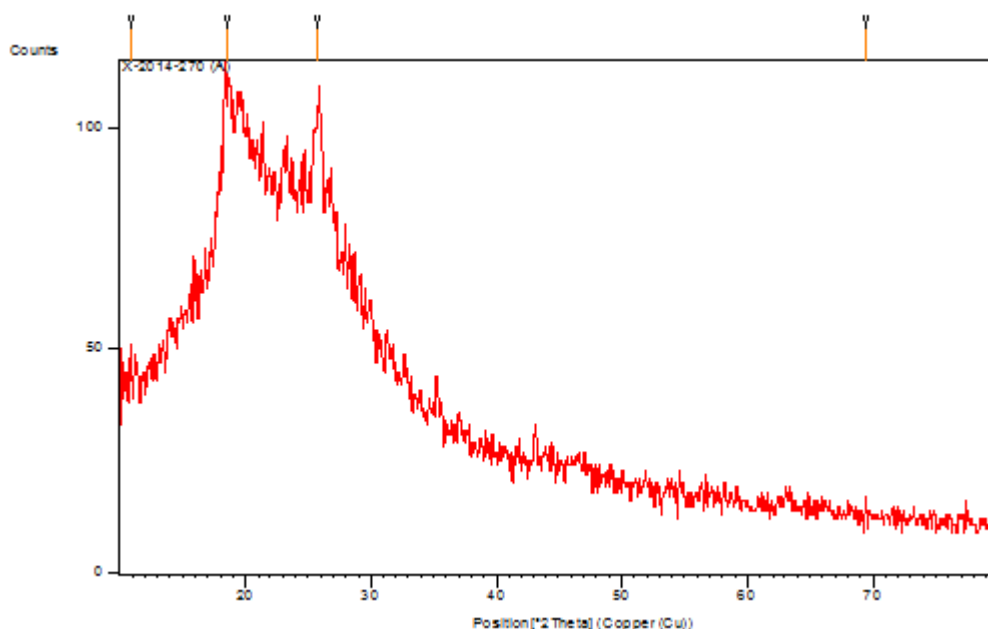


Figure 2: X-ray diffraction (XRD) patterns of the PANI nanoparticles.

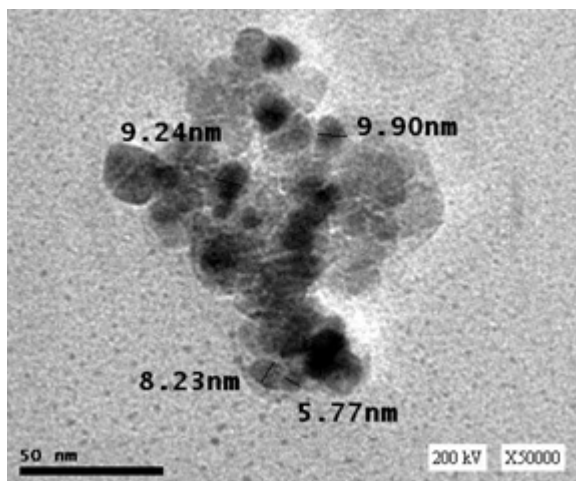


Figure 3: TEM image of polyaniline nanoparticles prepared by microemulsion polymerization

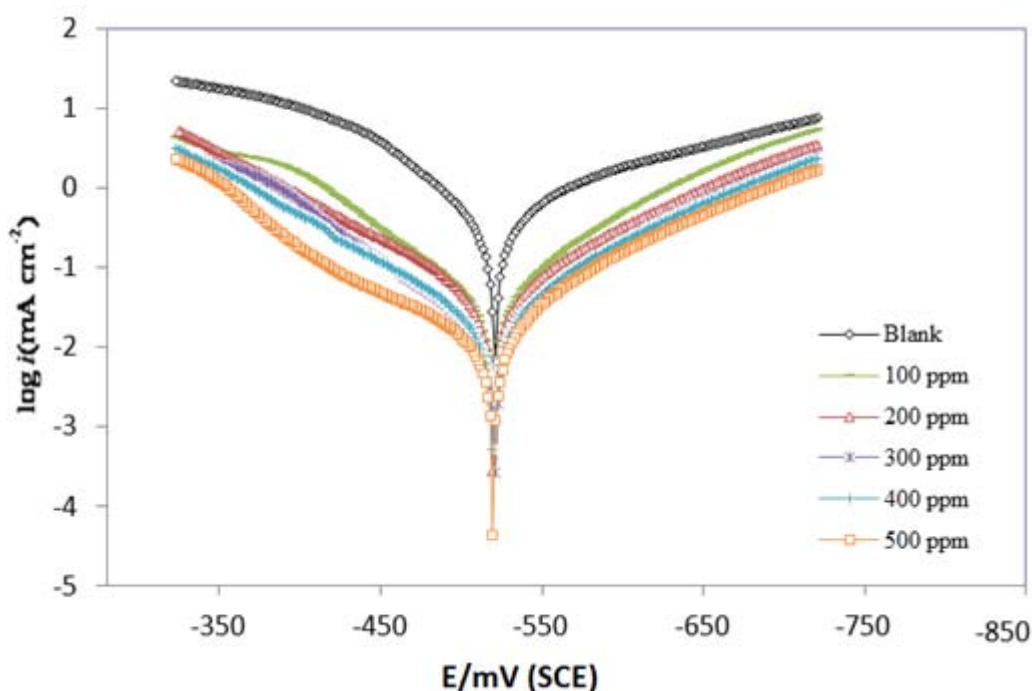


Figure 4: Potentiodynamic polarization curves for carbon steel in 1.0 M HCl containing different concentrations of nPAN at 30 °C.

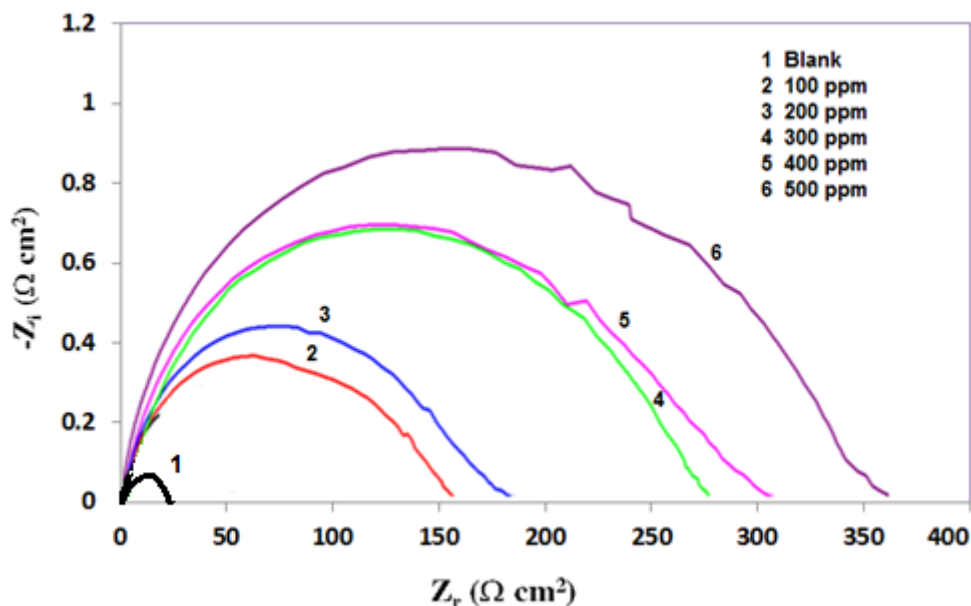


Figure 5: Nyquist plots for the carbon steel in 1 M HCl in absence and presence of different concentrations of nPAN.

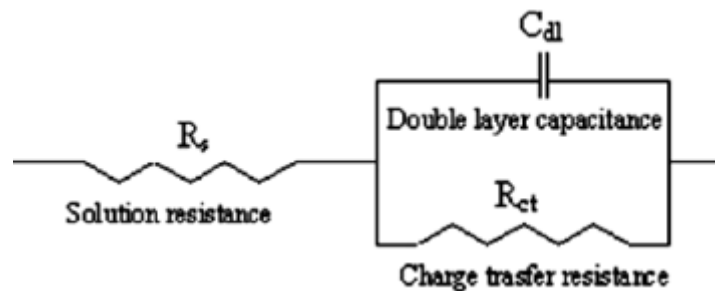


Figure 6: Suggested equivalent circuit model for the studied system.

Table 1: Potentiodynamic electrochemical parameters for the corrosion of steel in 1M HCl solution in the absence and presence different conc. of the investigated inhibitors at 30°C

Inhibitor	Concentration, ppm	$-E_{corr}$ , mV vs. SCE	$I_{corr}$ , mA cm <sup>-2</sup>	$\beta_a$ , mV dec <sup>-1</sup>	$-\beta_c$ , mV dec <sup>-1</sup>	$\eta_p$ , %
nPAN	0	-530.8	0.821	158.9	-164.9	0
	100	-519.5	0.123	123.9	-145.6	85.01
	200	-525.7	0.093	108.8	-121.1	88.67
	300	-522.3	0.07	100.4	-120.4	91.47
	400	-520.4	0.063	98.4	-87.7	92.32
	500	-521.8	0.0542	101.0	-89.3	93.39

Table 2: EIS parameters for corrosion of carbon steel in 1M HCl in absence and presence of different concentration of the nPAN at 30°C

Inhibitor	Conc. of inhibitor	$R_s$ (ohm cm <sup>2</sup> )	$R_{ct}$ (ohm cm <sup>2</sup> )	$C_{dl}$ (μF cm <sup>-2</sup> )	$\eta_i$ (%)
Blank	0	0.21	20	94.34	-
nPAN	100	0.08	160	95.61	87.5
	200	1.13	180	80.23	88.88
	300	0.74	280	52.13	92.85
	400	2.21	310	23.51	93.54
	500	1.14	370	17.39	94.59